



HAL
open science

Estimation of joint contact pressure in the index finger using a hybrid finite element musculoskeletal approach

Barthélémy Faudot, Jean-Louis Milan, Benjamin Goislard de Monsabert,
Thomas Le Corroller, Laurent Vigouroux

► To cite this version:

Barthélémy Faudot, Jean-Louis Milan, Benjamin Goislard de Monsabert, Thomas Le Corroller, Laurent Vigouroux. Estimation of joint contact pressure in the index finger using a hybrid finite element musculoskeletal approach. *Computer Methods in Biomechanics and Biomedical Engineering*, 2020, 23 (15), pp.1225-1235. 10.1080/10255842.2020.1793965 . hal-03192663

HAL Id: hal-03192663

<https://hal.science/hal-03192663v1>

Submitted on 8 Apr 2021

HAL is a multi-disciplinary open access archive for the deposit and dissemination of scientific research documents, whether they are published or not. The documents may come from teaching and research institutions in France or abroad, or from public or private research centers.

L'archive ouverte pluridisciplinaire **HAL**, est destinée au dépôt et à la diffusion de documents scientifiques de niveau recherche, publiés ou non, émanant des établissements d'enseignement et de recherche français ou étrangers, des laboratoires publics ou privés.



Estimation of joint contact pressure in the index finger using a hybrid finite element musculoskeletal approach

| | |
|-------------------------------|---|
| Journal: | <i>Computer Methods in Biomechanics and Biomedical Engineering</i> |
| Manuscript ID | GCMB-2020-0028 |
| Manuscript Type: | Research Article (4,000 words) |
| Date Submitted by the Author: | 17-Jan-2020 |
| Complete List of Authors: | Faudot, Barthélémy; Aix-Marseille Université, Institute of Movement Sciences Milan, Jean-Louis; Aix-Marseille Université, Institute of Movement Sciences Goislard de Monsabert, Benjamin; Aix-Marseille Université, Institute of Movement Sciences Le Corroller, Thomas; Aix-Marseille Université, Institute of Movement Sciences; Assistance Publique Hôpitaux de Marseille, Institute for Locomotion - Department of Radiology - St Marguerite Hospital Vigorous, Laurent; Aix-Marseille Université, Institute of Movement Sciences |
| Keywords: | Hand biomechanics, joint contact pressure, pinch grip task, finite element analysis, musculoskeletal model |
| | |

SCHOLARONE™
Manuscripts

Estimation of joint contact pressure in the index finger using a hybrid finite element musculoskeletal approach

Barthélémy Faudot^{a*}, Jean-Louis Milan^a, Benjamin Goislard de Monsabert^a,
Thomas Le Corroller^{a,b}, Laurent Vigouroux^a

^a*Aix Marseille University, CNRS, ISM, Marseille, France*

^b*APHM, Institute for Locomotion, Department of Radiology, St Marguerite Hospital, Marseille, France*

*Corresponding Author

Barthélémy Faudot

Faculty of Sport Science, CP 910

Institute of Movement Science

163 Avenue de Luminy

13288 Marseille Cedex 09 (France)

Email: barthelemy.faudot@univ-amu.fr

Tel: +33(0)4 91 75 96 55

Fax: +33(0)4 91 17 22 52

Estimation of joint contact pressure in the index finger using a hybrid finite element musculoskeletal approach

Abstract

The knowledge of local stress distribution in hand joints, in particular joint contact pressure, is crucial to understand injuries and osteoarthritis occurrence. However, determining cartilage contact stresses remains a challenge, requiring numerical models including both accurate anatomical components and realistic tendon force actuation. Contact forces in finger joints have frequently been calculated but little data is available on joint contact pressures. This study aimed to develop and validate a hybrid biomechanical model of the index finger to estimate in-vivo joint contact pressure during a static maximal strength pinch grip task. The hybrid model employed a two-step approach. First, a three-dimensional finite element model including bones, cartilage, tendons and ligaments was developed, with tendon force transmission based on a tendon-pulley system. Then, this model was driven by realistic tendon forces estimated from a musculoskeletal model and motion capture data for six subjects. The hybrid model outputs agreed well with experimental measurement of fingertip forces and musculoskeletal model results. Mean contact pressures were 8.0 ± 1.4 MPa, 7.0 ± 1.3 MPa and 7.2 ± 2.6 MPa for metacarpophalangeal, proximal and distal interphalangeal joints, respectively. Two subjects had higher mean contact pressure in the distal joint than in the two other joints, suggesting a mechanical cause for the prevalence of osteoarthritis in the index distal joint. This first application of an effective hybrid model to the index finger holds promise for estimating hand joint stresses under common daily grip tasks. Knowledge of comprehensive hand biomechanics is of major clinical interest to provide the numerical groundwork to improve surgical procedures.

Keywords

Hand biomechanics, joint contact pressure, pinch grip task, finite element analysis, musculoskeletal model

Introduction

The human hand is a sophisticated biological tool involved in numerous everyday activities (Bardo et al. 2018). The gripping tasks performed by the hand are essential for most movements in daily and working life. One of the commonest of the various techniques (e.g.: cylindrical, key pinch, hook grip) (Napier 1956) used to manipulate objects is the pinch grip, which consists in holding an object between the thumb and the index fingertips (Vergara et al. 2014). Because of its specific biomechanical configuration, this grip technique can lead to high joint loadings that expose the fingers to injuries such as rheumatoid arthritis and osteoarthritis (OA) (Jensen et al. 1999; McQuillan et al. 2016). Cumulative excessive stress acting on normal joints has in fact been identified as one of the main risk factors for the development of OA (Guilak 2011; Buckwalter et al. 2013). Hence, quantifying the biomechanical stress distribution on the finger's musculoskeletal system, especially joint contact pressure, could provide a better understanding of joint disease (Goislard de Monsabert et al. 2014) and improve rehabilitation (Fowler & Nicol 2000; Completo et al. 2018).

Direct measurements of joint pressures have been estimated in-vivo using pressure sensors (Rikli et al. 2007) and instrumented prostheses for large joints (D'Lima et al. 2006). However, the highly invasive nature of such techniques makes them ethically questionable and a technical challenge, especially when applied to the small finger joints. Only a few in vitro experimental data for the hand are available, due to the joint size and to the surrounding tissues that complicate the insertion of such sensors. Therefore, computational modelling, being non-invasive, appears to be the most suitable method of estimating joint mechanics.

Finite element (FE) and musculoskeletal (MSK) are the main modelling approaches currently used to study joint loadings (Henak et al. 2013). They have been widely applied to the lower limb during isometric tasks (Cheung et al. 2005) and gait locomotion (Andriacchi et al. 2009) to estimate either joint kinematics, reaction forces or joint cartilage stress. Due to the number of anatomical components involved and the complexity of soft-tissue interaction, multi-

1
2
3 articular systems such as the finger, wrist or ankle have received less attention. Most hand
4
5 biomechanical models use an MSK representation for either the index finger (Fowler & Nicol
6
7 2000; Synek & Pahr 2016), the thumb-index pinch complex (Barry et al. 2018) or the entire
8
9 hand (Goislard de Monsabert et al. 2014). Although such models provide estimations of tendon
10
11 forces and resultant joint contact forces, they neglect the non-linear deformation of soft tissues
12
13 and the local stress distribution. Conversely, FE hand models provide estimations of local
14
15 contact mechanics but focus on a single joint (Hashizume et al. 1994), model joints in 2D (Butz
16
17 et al. 2012a), neglect muscle actions and tendon paths (Butz et al. 2012b) and apply non-
18
19 physiological boundary conditions (Hariri 2019). To take advantage of both approaches, hybrid
20
21 MSK-FE models have been developed to investigate different musculoskeletal structures, such
22
23 as the wrist (Gislason et al. 2010), the ankle (Wang et al. 2016) or the knee (Besier et al. 2005;
24
25 Halonen et al. 2017). However, the implementation of this hybrid approach remains challenging
26
27 when modelling the hand, whose multi-joint configuration makes it particularly difficult to
28
29 validate the numerical procedure.
30
31
32
33

34
35 A hybrid MSK-FE model representing bones, cartilage, tendons, annular pulleys and ligaments
36
37 while considering the multi-joint actions of tendons would help to improve the understanding
38
39 of musculoskeletal diseases. To the best of our knowledge, no studies have so far applied this
40
41 hybrid approach to the hand joints. Thus, the purpose of this paper was to provide a validated
42
43 hybrid biomechanical model of the index finger that estimates in-vivo joint contact pressure by
44
45 applying realistic muscle actions during a static maximal strength pinch grip task.
46
47
48
49
50

51 **Methods**

52
53 The workflow of the study is presented in Fig. 1. This hybrid approach combined an already
54
55 published MSK model based on experimental data with a newly developed FE model of the
56
57 index finger based on medical imaging and literature data. The MSK model estimated tendon
58
59
60

1
2
3 forces from kinematic and force data through an inverse dynamic approach. Tendon forces were
4
5 then inputted into the FE model and joint contact pressures were computed.
6

7
8 *[Figure 1 about here]*
9

10 ***Experimental kinematic and force data***

11
12 The experimental setup and protocol already reported (Goislard de Monsabert et al. 2014) are
13
14 briefly described here. Ten healthy right-handed males free of upper extremity disorders were
15
16 recruited (age: 25.5 ± 3.2 years; height: 178.6 ± 6.1 cm; weight: 71.2 ± 7.2 kg; hand length:
17
18 19.0 ± 0.8 cm). Kinematic and force data (Fig. 2) were simultaneously recorded. A six-axial
19
20 force sensor (Nano-25; ATI Industrial Automation, USA) 5.5 cm long was used to record the
21
22 force applied by the thumb and index fingertips. The 3D position of hand segments was tracked
23
24 using spherical reflecting markers and a six-camera optoelectronic system (MX T40; Vicon,
25
26 UK). Joint angles and the three grip force components were then inputted into the MSK model.
27
28
29

30
31 *[Figure 2 about here]*
32

33 ***Tendon force estimation using a musculoskeletal model***

34
35 A full description of the MSK model is provided in a previous study (Goislard de Monsabert et
36
37 al. 2012). The model estimated 42 tendon forces to balance 23 degrees of freedom (DoF)
38
39 representing the five fingers and the wrist. The segments were modelled as rigid bodies
40
41 articulated by sixteen frictionless joints. In the first step, the 42 tendon forces required to
42
43 balance external forces were estimated using a static optimisation to solve the muscular
44
45 redundancy problem. In the second step, joint reaction forces were derived from tendon and
46
47 external fingertip forces using the force equilibrium equation.
48
49

50 51 ***Finite element model***

52 ***Model geometry***

53
54
55 A healthy male subject free of upper extremity disorders was recruited to acquire computed
56
57 tomography (CT) images of the right hand (age: 37 years; height: 185 cm; weight: 74 kg; hand
58
59
60

length: 19.7 cm). The participant signed an informed consent form and the protocol was approved by the local ethics committee. The CT system was a LightSpeed VCT (GE Medical Systems, USA) (150 mA x 120 kV; slice thickness 625 μm ; pixel size 325 μm). The subject placed his hand in a semi-rigid cast that constrained him in a pinch grip posture. The cast was made prior to the acquisition to avoid any effect of fatigue. Polyurethane resin tapes (Soft Cast, 3M, USA) were positioned while the subject was holding a 5.5 cm-long tube, i.e. the same length as the force sensor.

Segmentation of bones was performed from the CT-scan acquisition using the 3D image reconstruction software Mimics (Research 20.0; Materialise, Belgium). Index phalanges and truncated metacarpal bone were meshed using quadratic tetrahedral elements (C3D10) with a maximum element edge length of 1.5 mm. Solid geometries were imported into Abaqus (2018; Simulia, USA). The cartilage was manually created by identifying joint surfaces on bones and then extruding surface elements to form two-layer wedge elements (C3D6), each of whose widths equalled half the minimum distance between bones (Anderson et al. 2010). Cartilage distribution and thickness (from 0.4 to 0.8 mm) were compared against literature values (Robson et al. 1995). The FE model's total number of elements was roughly 200 000.

Modelling tissue properties

Finger bones were modelled as a linear elastic isotropic material, distinguishing between cortical ($E=18$ GPa, $\nu=0.2$) and cancellous bone ($E=300$ MPa, $\nu=0.25$) (Rho et al. 1997), see Fig. 3(B). Cartilage was modelled using a 3rd order Ogden hyper-elastic material as detailed in Table 1. Supplementary analysis was performed to investigate the effect of bone material properties on the model results.

All the tendons and muscles involved in index finger function were modelled: *terminal extensor*, *flexor digitorum profundus* (FDP) at distal interphalangeal (DIP) joint, *extensor slip*, *radial band*, *ulnar band*, *flexor digitorum superficialis* (FDS) at proximal interphalangeal (PIP)

1
2
3 joint and *long extensor* (considering both *extensor digitorum communis* (EDC) and *extensor*
4 *digitorum indicis* (EDI)), *radial interosseus* (RI), *ulnar interosseus* (UI), *lumbrical* (LU) at
5
6 metacarpophalangeal (MCP) joint. The paths of these tendons were determined by the same
7
8 anatomical and geometrical data in the MSK model and scaled according to phalange
9
10 dimensions (An et al. 1979). Each tendon was modelled using straight beams (B31) to connect
11
12 the points given by the anatomical dataset, i.e. two points at each joint. Tendons were held tight
13
14 to the bone by annular pulleys modelled with shell elements (S4) for both flexor and extensor
15
16 tendons (see Fig. 3).
17
18
19
20

21 Collateral ligaments and volar plates were modelled as the main stabilisers of the index finger
22
23 joints (Minami et al. 1985). The same attachment points as those used for the MSK model were
24
25 estimated from an anatomical study (An et al. 1979). Distributed insertions were simulated by
26
27 applying ligaments in parallel at adjacent node points on the bone surface. Ligaments were
28
29 modelled as non-linear spring elements (CONN3D2) with tension-only behaviour and pre-
30
31 strain at initial length (Rhee et al. 1992). Model values are summarised in Table 1.
32
33
34

35 *[Table 1 about here]*

36 *[Figure 3 about here]*

37 *Loads and boundary conditions*

38
39
40 Loadings on the hybrid model were driven through the estimation of tendon forces provided by
41
42 the MSK analysis previously described. Four of the ten subjects were excluded from the
43
44 analysis due to the large difference between their joint angles and those of the scanned subject.
45
46 For the six remaining subjects, tendon forces were applied to the end of each tendon in the
47
48 direction of the last beam segment (Fig. 3) and the six datasets were analysed. An extra
49
50 simulation was performed using the average value of tendon forces. Supplementary analysis
51
52 was also conducted to investigate the effect of tendon forces on the model results.
53
54
55
56
57
58
59
60

1
2
3 Bone and cartilage were fixed together so as to allow no relative motion between them. A
4 friction coefficient of 0.02 (Wright & Dowson 1976) was applied to each cartilage joint surface.
5
6

7 The proximal end of the truncated metacarpal bone was fully constrained and index fingertip
8 nodes were restricted to one DoF to model the contact with the force sensor (see Fig. 3).
9

10 The Abaqus explicit solver was used for the analysis, this algorithm making the contact model
11 robust.
12

13 *Verification and validation of the hybrid model*

14

15 To validate the hybrid approach, several analyses were performed to assess the quality of the
16 hybrid model. First, the FE environment was evaluated through an assessment of the mesh
17 quality and the convergence criterion. Resultant fingertip forces estimated in the hybrid model
18 at the fixed fingertip nodes were compared to the experimental forces measured by the force
19 sensor. The ratio of inputted tendon forces to estimated fingertip forces provided by the hybrid
20 model for both FDP and FDS was compared to literature values. Lastly, the sum of reaction
21 forces for all nodes of each joint in the hybrid model was compared to the joint reaction forces
22 of the MSK model. These comparisons were performed using the average value of tendon
23 forces of the six subjects inputted into the hybrid model.
24
25
26
27
28
29
30
31
32
33
34
35
36
37
38
39
40
41

42 **Results**

43 *Results of the MSK model*

44

45 The MSK model results are summarised here, for a full description see (Goislard de Monsabert
46 et al. 2014). Tendon forces and averaged tendon force values for the six subjects are given in
47 Supplementary Material A. For flexor tendons, resulting tensions were 158.0 ± 82.2 N and
48 109.8 ± 41.0 for the FDP and FDS tendons, respectively. For the extensor mechanism, resulting
49 tensions were 5.1 ± 5.6 N, 181.2 ± 46.3 N, 0.0 ± 0.0 N, 85.6 ± 34.1 N, 110.0 ± 43.8 N for the
50 LU, RI, UI, EDC and EDI tendons, respectively.
51
52
53
54
55
56
57
58
59
60

Subjects gripped the object using a variety of finger postures. DIP, PIP, and MCP flexion angles ranged from 8.9° to 28.8°, -1.0° to 21.3° and 46.5° to 64.4°, respectively. The scanned subject had flexion angles of 9.3°, 16.9°, and 47.6° for DIP, PIP and MCP joints, respectively.

Finite element environment quality indicators

Mesh quality was checked against the recommendations of a previously published article (Burkhart et al. 2013), detailed in Table 2, ensuring that elements with poor mesh metrics were located far from areas of interest. The model converged, at the end of the load step, with a mean kinetic energy of 3.4% of the total strain energy. Any dynamic behaviour was excluded according to the literature (Choi et al. 2002), leading to a quasi-static simulation.

[Table 2 about here]

Validation of the hybrid model

The hybrid model outputs agreed well with experimental and MSK model results. The fingertip reaction force estimated by the hybrid model using averaged tendon force was 54.8 N, lower than the experimental measurement by the force sensor, but remained within one standard deviation (66.2 ± 13.3 N). The hybrid model estimated a tendon force to external fingertip force ratio of 1.85 and 2.67 for FDP and FDS, respectively, as shown in Table 3. The joint reaction forces estimated by the hybrid model were higher than those of the MSK model but remained within one standard deviation. The sum of DIP, PIP and MCP joint reaction forces was 758.2 N, 481.7 N and 248.7 N, respectively. The results are summarised in Table 4.

[Table 3 about here]

[Table 4 about here]

Joint mechanical stresses estimated by the hybrid model

Joint contact pressure on cartilage surfaces and Von Mises stress distribution on bones of the index finger during a pinch grip task for one dataset of tendon forces are displayed in Fig. 4. The highest stress was found on the surface of the metacarpal bone. High stress-intensity

1
2
3 regions were visible at bone-pulley interface and at ligament insertions because of the node
4 coupling points (Fig. 4). However, these stresses were highly localised and not representative
5 of the real bone condition, being due to numerical artefacts. Finger joint contact areas were
6 computed by summing all the facets bearing contact force and yielded 53.4 ± 4.6 mm², 76.2 ± 5.1
7 mm² and 94.8 ± 2.1 mm² for DIP, PIP and MCP joints, respectively. Maximal contact pressure
8 on cartilage was computed as well as mean contact pressure by averaging pressure values on
9 the contact area at each joint (Fig.4). For DIP, PIP, and MCP joints, maximal contact pressure
10 was 30.3 ± 8.2 MPa, 31.9 ± 8.8 MPa, and 33.8 ± 6.9 MPa and mean contact pressure was 7.2 ± 2.6
11 MPa, 7.0 ± 1.3 MPa, and 8.0 ± 1.4 MPa, respectively, as shown in Table 5.
12
13
14
15
16
17
18
19
20
21
22

23
24 *[Table 5 about here]*

25
26 *[Figure 4 about here]*

27 28 ***Sensitivity analysis***

29
30 The sensitivity analysis on material properties showed that considering bones as rigid or
31 homogeneous elastic solid tended to increase joint contact pressure. On sensitivity to tendon
32 force, the results showed that joint contact pressure and external fingertip force decreased
33 linearly with tendon force intensity. Further details can be found in Supplementary Material B.
34
35
36
37
38
39
40
41

42 43 **Discussion**

44 We described here the development of a hybrid biomechanical model of the index finger to
45 estimate joint contact pressure during a static maximal strength pinch grip task in an FE
46 environment driven by tendon forces calculated by an MSK model. This method combines two
47 different numerical hand models to estimate joint mechanical stresses, notably mean and
48 maximal joint contact pressures. This highly innovative approach represents, to the best of our
49 knowledge, the first attempt to apply and validate a multi-articular hybrid model to the hand
50 joints.
51
52
53
54
55
56
57
58
59
60

1
2
3 When evaluated through a combination of sensitivity analysis and comparison with
4 experimental measurements, MSK results and literature data, the hybrid model was shown to
5 provide realistic estimation of hand loadings. First, the estimated fingertip reaction force was
6 in good agreement with the experimental grip force recorded using the force sensor, with only
7 a 17% difference stable across subjects. The consistency of this gap suggests that its origin lies
8 in the use of a single bone geometry in the hybrid model, whereas the experimental gripping
9 task involved six subjects, each with a different bone geometry. There was good agreement in
10 resultant joint reaction forces between the hybrid and the MSK models, both of which showed
11 an increase from distal to proximal joints and a major difference at the DIP joint. The negligible
12 differences between the hybrid and the MSK model may be explained by the use of different
13 assumptions in the two numerical approaches, such as non-deformable bodies in the MSK
14 model versus a more accurate representation of bone and cartilage in the hybrid model. Lastly,
15 joint contact areas predicted in the hybrid model showed similar values to those of the MSK
16 model and literature data (Moran et al. 1985).

17
18
19
20
21
22
23
24
25
26
27
28
29
30
31
32
33
34
35
36
37
38
39
40
41
42
43
44
45
46
47
48
49
50
51
52
53
54
55
56
57
58
59
60
The hybrid model proposes a new tendon force transmission based on a tendon-pulley system,
where both flexor and extensor tendons slid in annular pulleys. This yielded estimations of the
ratio of flexor tendon forces to fingertip force that were consistent with in-vivo measurements
found in the literature (Schuind et al. 1992; Dennerlein et al. 1998; Kurasa et al. 2005) and with
MSK results, thus validating this approach (Table 3). In a previous study (Harish 2019), the DIP
joint was driven by a concentrated force at the end of a wire connector which modelled the
distal part of the flexor tendon. The same approach has been used in some foot FE models
(Isvilanonda et al. 2012; Morales-Orcajo et al. 2015; Wang et al. 2016), with tendons crossing
several joints and the tendon final insertion attached to the bone.

The choice of material properties in the hybrid model was based on several factors. Sensitivity
analysis (see Supplementary Material B) showed that bone representation had an impact on

1
2
3 joint contact pressures. Distinguishing between cortical and cancellous bone ensured here that
4
5 the structure was rigid enough for good transmission of stresses between cartilage layers and
6
7 bones. This suggests that piecewise assigning of linear-elastic material properties to bones, by
8
9 calculating the density of the CT-scan gray value of each element, better matches the real
10
11 microarchitecture of the bone. Cartilage was represented here as a monophasic time-
12
13 independent hyperelastic material that could handle large deformations greater than 5%.
14
15 Although this did not account for either poroelastic behaviour or fluid matrix interactions such
16
17 as osmotic swelling or mechanical exudation of interstitial fluid (Halloran et al. 2012),
18
19 hyperelastic models are deemed adequate to characterise the equilibrium response of cartilage
20
21 (Brown et al. 2009).
22
23
24

25
26 The calculation of mean contact pressures for the maximal strength grip task performed by six
27
28 subjects showed significant differences among them. For two subjects (4 and 9), mean contact
29
30 pressures resulted in greater values for the DIP joint than for PIP and MCP joints. For the index
31
32 finger, several studies have shown that OA is more frequent in the DIP joint than in the proximal
33
34 joints (Caspi et al. 2001; Dahaghin et al. 2005). It can therefore be concluded that cumulative
35
36 excessive stresses acting on joints should lead to the occurrence and development of OA,
37
38 consistent with previous findings (Guilak 2011; Buckwalter et al. 2013). In contrast, the
39
40 remaining four subjects (1, 2, 3 and 7) showed higher mean contact pressures in the MCP joint
41
42 than in the PIP and DIP joints. Studies have found that the MCP joint is the most subject to OA
43
44 development during maximal strength tasks (Jensen et al. 1999), while the DIP joint is the most
45
46 sensitive under precision repetitive grip tasks (Lehto et al. 1990). Furthermore, to perform the
47
48 maximal strength grip task, different neuromuscular strategies were employed by the subjects.
49
50 Since these strategies activated the muscles in varying ways, they resulted in varying joint
51
52 contact pressures. In subjects 4 and 9, greater mean contact pressures at the distal joint were
53
54 induced by higher FDP muscular activity resulting in higher FDP tendon force. In subject 7,
55
56
57
58
59
60

1
2
3 greater mean contact pressures at proximal and metacarpophalangeal joints were due to higher
4
5 FDS and RI muscular activities resulting in higher FDS and RI tendon forces.
6

7
8 The mean contact pressures obtained in the hybrid simulation reached 8.0 ± 1.4 MPa at the MCP
9
10 joint (Table 5), which could indicate tissue consolidation. Indeed, this value was in the range
11
12 of those moderate normal loadings needed for cartilage development and renewal, and to
13
14 maintain functional integrity (Vanwanseele et al. 2002), thus keeping cartilage healthy
15
16 (Parkkinen et al. 1992; Clements et al. 2001). However, peak contact pressures at DIP, PIP and
17
18 MCP joints (higher than 15 MPa) corresponded to an excessive mechanical load which could
19
20 therefore cause chondrocyte death and extracellular matrix damage (Torzilli et al. 1999), thus
21
22 leading to OA initiation. It should be noted that this study examined an extreme force intensity
23
24 of one of the most common techniques for manipulating objects, the pinch grip. While a pinch
25
26 strength of 10 N will actually suffice for 90% of daily living activities (Hunter et al. 1978), the
27
28 simulated pinch strength here was more than 5 times higher, with an experimental fingertip
29
30 force of 66.2 ± 13.3 N. Thus, the task studied here could be considered as a worst-case for
31
32 which the conditions of OA occurrence were assessed and evaluated.
33
34
35

36
37 The hybrid method presented in this article offers access to individual subjects' local stress
38
39 distribution in index finger joints through a non-invasive evaluation. It can be applied and
40
41 extended to the complete hand to simulate tasks such as the power grip and to potentially link
42
43 the mechanical determinants and consequences of diseases such as OA. A deeper understanding
44
45 of the biomechanics of the hand related to joint disease occurrence could provide the
46
47 groundwork to improve surgical procedures, such as arthroplasty, through more effective
48
49 numerical models.
50
51

52 53 **Acknowledgment**

54
55 The authors wish to thank André Jacques for his assistance with the numerical simulations.
56
57

58 59 **Conflict of Interest Statement**

60

1
2
3 No benefits in any form have been or will be received from a commercial party related directly
4
5 or indirectly to the subject of this manuscript.
6
7
8
9
10
11
12
13
14
15
16
17
18
19
20
21
22
23
24
25
26
27
28
29
30
31
32
33
34
35
36
37
38
39
40
41
42
43
44
45
46
47
48
49
50
51
52
53
54
55
56
57
58
59
60

For Peer Review Only

References

- An KN, Chao EY, Cooney WP, Linscheid RL. 1979. Normative model of human hand for biomechanical analysis. *J Biomech.* 12(10):775–788.
- Anderson AE, Ellis BJ, Maas SA, Weiss JA. 2010. Effects of idealized joint geometry on finite element predictions of cartilage contact stresses in the hip. *J Biomech.* 43(7):1351–1357.
- Andriacchi TP, Koo S, Scanlan SF. 2009. Gait mechanics influence healthy cartilage morphology and osteoarthritis of the knee. *J Bone Joint Surg Am.* 91 Suppl 1:95–101.
- Bardo A, Vigouroux L, Kivell TL, Pouydebat E. 2018. The impact of hand proportions on tool grip abilities in humans, great apes and fossil hominins: A biomechanical analysis using musculoskeletal simulation. *J Hum Evol.* 125:106–121.
- Barry AJ, Murray WM, Kamper DG. 2018. Development of a dynamic index finger and thumb model to study impairment. *J Biomech.* 77:206–210.
- Besier TF, Gold GE, Beaupré GS, Delp SL. 2005. A modeling framework to estimate patellofemoral joint cartilage stress in vivo. *Med Sci Sports Exerc.* 37(11):1924–1930.
- Brown CP, Nguyen TC, Moody HR, Crawford RW, Oloyede A. 2009. Assessment of common hyperelastic constitutive equations for describing normal and osteoarthritic articular cartilage. *Proc Inst Mech Eng [H].* 223(6):643–652.
- Buckwalter JA, Anderson DD, Brown TD, Tochigi Y, Martin JA. 2013. The Roles of Mechanical Stresses in the Pathogenesis of Osteoarthritis: Implications for Treatment of Joint Injuries. *Cartilage.* 4(4):286–294.
- Burkhart TA, Andrews DM, Dunning CE. 2013. Finite element modeling mesh quality, energy balance and validation methods: a review with recommendations associated with the modeling of bone tissue. *J Biomech.* 46(9):1477–1488.
- Butz KD, Merrell G, Nauman EA. 2012a. A biomechanical analysis of finger joint forces and stresses developed during common daily activities. *Comput Methods Biomech Biomed Engin.* 15(2):131–140.
- Butz KD, Merrell G, Nauman EA. 2012b. A three-dimensional finite element analysis of finger joint stresses in the MCP joint while performing common tasks. *HAND.* 7(3):341–345.
- Caspi D, Flusser G, Farber I, Ribak J, Leibovitz A, Habet B, Yaron M, Segal R. 2001. Clinical, radiologic, demographic, and occupational aspects of hand osteoarthritis in the elderly. *Semin Arthritis Rheum.* 30(5):321–331.
- Cheung JT-M, Zhang M, Leung AK-L, Fan Y-B. 2005. Three-dimensional finite element analysis of the foot during standing—a material sensitivity study. *J Biomech.* 38(5):1045–1054.
- Choi H-H, Hwang S-M, Kang YH, Kim J, Kang BS. 2002. Comparison of Implicit and Explicit Finite-Element Methods for the Hydroforming Process of an Automobile Lower Arm. *Int J Adv Manuf Technol.* 20(6):407–413.
- Clements KM, Bee ZC, Crossingham GV, Adams MA, Sharif M. 2001. How severe must repetitive loading be to kill chondrocytes in articular cartilage? *Osteoarthritis Cartilage.* 9(5):499–507.
- Completo A, Nascimento A, Girão AF, Fonseca F. 2018. Biomechanical evaluation of pyrocarbon proximal interphalangeal joint arthroplasty: An in-vitro analysis. *Clin Biomech Bristol Avon.* 52:72–78.
- Dahaghin S, Bierma-Zeinstra SMA, Ginai AZ, Pols H a. P, Hazes JMW, Koes BW. 2005. Prevalence and pattern of radiographic hand osteoarthritis and association with pain and disability (the Rotterdam study). *Ann Rheum Dis.* 64(5):682–687.
- Dennerlein JT, Diao E, Mote CD, Rempel DM. 1998. Tensions of the flexor digitorum superficialis are higher than a current model predicts. *J Biomech.* 31(4):295–301.
- D’Lima DD, Patil S, Steklov N, Slamin JE, Colwell CW. 2006. Tibial Forces Measured In Vivo After Total Knee Arthroplasty. *J Arthroplasty.* 21(2):255–262.
- Fowler NK, Nicol AC. 2000. Interphalangeal joint and tendon forces: normal model and biomechanical consequences of surgical reconstruction. *J Biomech.* 33(9):1055–1062.
- Gíslason MK, Stansfield B, Nash DH. 2010. Finite element model creation and stability considerations of complex biological articulation: The human wrist joint. *Med Eng Phys.* 32(5):523–531.
- Goislard de Monsabert B, Rossi J, Berton E, Vigouroux L. 2012. Quantification of hand and forearm muscle forces during a maximal power grip task. *Med Sci Sports Exerc.* 44(10):1906–1916.

- 1
2
3 Goislard de Monsabert B, Vigouroux L, Bendahan D, Berton E. 2014. Quantification of finger joint loadings using
4 musculoskeletal modelling clarifies mechanical risk factors of hand osteoarthritis. *Med Eng Phys.* 36(2):177–184.
5
6 Guilak F. 2011. Biomechanical factors in osteoarthritis. *Best Pract Res Clin Rheumatol.* 25(6):815–823.
7
8 Halloran JP, Sibole S, van Donkelaar CC, van Turnhout MC, Oomens CWJ, Weiss JA, Guilak F, Erdemir A. 2012.
9 Multiscale mechanics of articular cartilage: potentials and challenges of coupling musculoskeletal, joint, and
10 microscale computational models. *Ann Biomed Eng.* 40(11):2456–2474.
11
12 Halonen KS, Dzialo CM, Mannisi M, Venäläinen MS, de Zee M, Andersen MS. 2017. Workflow assessing the
13 effect of gait alterations on stresses in the medial tibial cartilage - combined musculoskeletal modelling and finite
14 element analysis. *Sci Rep [Internet].* [accessed 2018 Sep 21] 7(1). <http://www.nature.com/articles/s41598-017-17228-x>
15
16 Harih G. 2019. Development of a Tendon Driven Finger Joint Model Using Finite Element Method. In: Cassenti
17 DN, editor. *Adv Hum Factors Simul Model [Internet].* Vol. 780. Cham: Springer International Publishing;
18 [accessed 2018 Sep 27]; p. 463–471. http://link.springer.com/10.1007/978-3-319-94223-0_44
19
20 Hashizume H, Akagi T, Watanabe H, Inoue H, Ogura T. 1994. Stress Analysis of PIP Joints using the Three-
21 Dimensional Finite Element Method. In: Schuind F, An KN, Cooney WP, Garcia-Elias M, editors. *Adv Biomech*
22 *Hand Wrist [Internet].* Boston, MA: Springer US; [accessed 2018 Sep 27]; p. 237–244.
23 http://link.springer.com/10.1007/978-1-4757-9107-5_21
24
25 Henak CR, Anderson AE, Weiss JA. 2013. Subject-specific analysis of joint contact mechanics: application to the
26 study of osteoarthritis and surgical planning. *J Biomech Eng.* 135(2):021003.
27
28 Hunter J, Schneider L, Mackin E, Bell J. 1978. *Rehabilitation of the hand.* St Louis: Mosby.
29
30 Isvilanonda V, Dengler E, Iaquinto JM, Sangeorzan BJ, Ledoux WR. 2012. Finite element analysis of the foot:
31 model validation and comparison between two common treatments of the clawed hallux deformity. *Clin Biomech*
32 *Bristol Avon.* 27(8):837–844.
33
34 Jensen V, Bøggild H, Johansen JP. 1999. Occupational use of precision grip and forceful gripping, and arthrosis
35 of finger joints: a literature review. *Occup Med Oxf Engl.* 49(6):383–388.
36
37 Kursk K, Diao E, Lattanza L, Rempel D. 2005. In vivo forces generated by finger flexor muscles do not depend
38 on the rate of fingertip loading during an isometric task. *J Biomech.* 38(11):2288–2293.
39
40 Lehto TU, Rönnemaa TE, Aalto TV, Helenius HY. 1990. Roentgenological arthrosis of the hand in dentists with
41 reference to manual function. *Community Dent Oral Epidemiol.* 18(1):37–41.
42
43 McQuillan TJ, Kenney D, Crisco JJ, Weiss A-P, Ladd AL. 2016. Weaker Functional Pinch Strength Is Associated
44 With Early Thumb Carpometacarpal Osteoarthritis. *Clin Orthop.* 474(2):557–561.
45
46 Minami A, An KN, Cooney WP, Linscheid RL, Chao EY. 1985. Ligament stability of the metacarpophalangeal
47 joint: a biomechanical study. *J Hand Surg.* 10(2):255–260.
48
49 Morales-Orcajo E, Bayod J, Becerro-de-Bengoa-Vallejo R, Losa-Iglesias M, Doblare M. 2015. Influence of first
50 proximal phalanx geometry on hallux valgus deformity: a finite element analysis. *Med Biol Eng Comput.*
51 53(7):645–653.
52
53 Moran JM, Hemann JH, Greenwald AS. 1985. Finger joint contact areas and pressures. *J Orthop Res Off Publ*
54 *Orthop Res Soc.* 3(1):49–55.
55
56 Napier JR. 1956. THE PREHENSILE MOVEMENTS OF THE HUMAN HAND. *J Bone Joint Surg Br.* 38-
57 B(4):902–913.
58
59 Parkkinen JJ, Lammi MJ, Helminen HJ, Tammi M. 1992. Local stimulation of proteoglycan synthesis in articular
60 cartilage explants by dynamic compression in vitro. *J Orthop Res Off Publ Orthop Res Soc.* 10(5):610–620.
Rhee RY, Reading G, Wray RC. 1992. A biomechanical study of the collateral ligaments of the proximal
interphalangeal joint. *J Hand Surg.* 17(1):157–163.
Rho JY, Tsui TY, Pharr GM. 1997. Elastic properties of human cortical and trabecular lamellar bone measured by
nanoindentation. *Biomaterials.* 18(20):1325–1330.
Rikli DA, Honigsmann P, Babst R, Cristalli A, Morlock MM, Mittlmeier T. 2007. Intra-articular pressure
measurement in the radioulnocarpal joint using a novel sensor: in vitro and in vivo results. *J Hand Surg.* 32(1):67–
75.
Robson MD, Hodgson RJ, Herrod NJ, Tyler JA, Hall LD. 1995. A combined analysis and magnetic resonance
imaging technique for computerised automatic measurement of cartilage thickness in the distal interphalangeal
joint. *Magn Reson Imaging.* 13(5):709–718.

- 1
2
3 Schuind F, Garcia-Elias M, Cooney WP, An KN. 1992. Flexor tendon forces: in vivo measurements. *J Hand Surg.* 17(2):291–298.
- 4
5 Synek A, Pahr DH. 2016. The effect of the extensor mechanism on maximum isometric fingertip forces: A
6 numerical study on the index finger. *J Biomech.* 49(14):3423–3429.
- 7
8 Torzilli PA, Grigiene R, Borrelli J, Helfet DL. 1999. Effect of impact load on articular cartilage: cell metabolism
9 and viability, and matrix water content. *J Biomech Eng.* 121(5):433–441.
- 10
11 Vanwansseele B, Eckstein F, Knecht H, Stüssi E, Spaepen A. 2002. Knee cartilage of spinal cord–injured patients
12 displays progressive thinning in the absence of normal joint loading and movement. *Arthritis Rheum.* 46(8):2073–
2078.
- 13
14 Vergara M, Sancho-Bru JL, Gracia-Ibáñez V, Pérez-González A. 2014. An introductory study of common grasps
15 used by adults during performance of activities of daily living. *J Hand Ther Off J Am Soc Hand Ther.* 27(3):225–
233; quiz 234.
- 16
17 Wang Y, Wong DW-C, Zhang M. 2016. Computational Models of the Foot and Ankle for Pathomechanics and
18 Clinical Applications: A Review. *Ann Biomed Eng.* 44(1):213–221.
- 19
20 Wright V, Dowson D. 1976. Lubrication and cartilage. *J Anat.* 121(Pt 1):107–118.
- 21
22
23
24
25
26
27
28
29
30
31
32
33
34
35
36
37
38
39
40
41
42
43
44
45
46
47
48
49
50
51
52
53
54
55
56
57
58
59
60

Figure Captions

Figure 1. Hybrid musculoskeletal-finite element model applied to the index finger for the estimation of joint contact pressure during a static maximal strength pinch grip task. The musculoskeletal model applied to six subjects estimated tendon and joint forces from motion capture and force data through an inverse dynamic approach. The finite element model based on medical imaging data and including all the major structures of the index finger was driven by tendon forces of the musculoskeletal model. This hybrid approach validated by comparison with experimental data and musculoskeletal results yielded mean and maximal contact pressures at the three index finger joints.

Figure 2. Pulp pinch grip posture and experimental acquisition system. A motion capture system with spherical markers on bony landmarks and an axial force sensor between the thumb and index fingertips were used.

Figure 3. (A) Index finger finite element model of the hybrid approach including bones, cartilage, tendons, annular pulleys and ligaments. Cartilage in green was obtained by extrusion of the bone surfaces with wedge elements. Tendons and annular pulleys in light blue and grey, respectively, were modelled with beam and shell elements, respectively. Ligaments in dark blue were represented by multiple non-linear spring elements. The truncated metacarpal bone was fully constrained and the fingertip restricted to one degree of freedom (DoF) resulting in an external fingertip reaction force (\vec{F}_{ext}). Datasets of tendon forces (\vec{F}_{musc}) were applied along the last segment of each tendon. (B) Material properties distribution between cortical (in light grey) and cancellous bone (in black) on a section of the index finger bones.

1
2
3 Figure 4. Von Mises stress distribution of the index finger and contact pressure distribution at
4 distal interphalangeal (DIP), proximal interphalangeal (PIP) and metacarpophalangeal (MCP)
5 joints during a static maximal strength pinch grip task applying one dataset of tendon forces.
6
7
8
9
10
11
12
13
14
15
16
17
18
19
20
21
22
23
24
25
26
27
28
29
30
31
32
33
34
35
36
37
38
39
40
41
42
43
44
45
46
47
48
49
50
51
52
53
54
55
56
57
58
59
60

For Peer Review Only

1
2
3 **Tables**
4
5

6 Table 1. Material properties and element types of the index finger hybrid finite element model
7

8

| 9 Component | Element type | Constitutive model | Constants |
|--------------------|------------------------|---|---|
| 11 Cortical bone | Tetrahedral | Linear elastic | E=18 GPa; $\nu=0.2$ |
| 13 Cancellous bone | Tetrahedral | Linear elastic | E=300 MPa; $\nu=0.25$ |
| 19 Cartilage | Wedge | Hyper-elastic 3 rd order Ogden | $\mu_1=-4527$; $\alpha_1=-4.98$ $\mu_2=2228$; $\alpha_2=5.43$ $\mu_3=2300$; $\alpha_3=4.55$ $D_1=D_2=D_3=0$ |
| 24 Tendons | Tension-only beam | Linear elastic | E=3 GPa; $\nu=0.3$ |
| 26 Pulleys | Shell | Linear elastic | E=1 GPa; $\nu=0.3$ |
| 28 Ligaments | Tension-only connector | Non-linear elastic | From 40 N/mm to 150 N/mm |

30
31
32
33
34
35
36
37
38
39
40
41
42
43
44
45
46
47
48
49
50
51
52
53
54
55
56
57
58
59
60

Table 2. Mesh quality metrics of the hybrid finite element model

| Mesh quality metric | Assessment criteria | Accurate elements |
|---------------------|---------------------|-------------------|
| Jacobian elements | > 0.2 | 94% |
| Aspect ratio | < 3 | 96% |
| Max angles | $< 120^\circ$ | 99% |

For Peer Review Only

Table 3. Comparison of ratios of tendon force to external fingertip force during pinch grip between MSK model, hybrid model and in-vivo measurements reported in the literature

| | FDP | FDS |
|-------------------|---------------|---------------|
| MSK model | 1.7 | 2.4 |
| Hybrid model | 2.0 | 2.9 |
| Schuind et al. | 7.9 ± 6.3 | 1.7 ± 1.5 |
| Denenrlein et al. | -- | 3.3 ± 1.4 |
| Kursa et al. | 2.4 ± 0.7 | 1.5 ± 1.0 |

1
2
3 Table 4. Force values obtained from musculoskeletal and hybrid models of the index finger.
4
5 External fingertip force and joint reaction force in distal interphalangeal (DIP), proximal
6
7 interphalangeal (PIP) and metacarpophalangeal (MCP) joints from the two models are
8
9 compared.
10
11

| | External fingertip force (N) | DIP joint reaction force (N) | PIP joint reaction force (N) | MCP joint reaction force (N) |
|--------------|---------------------------------|---------------------------------|---------------------------------|---------------------------------|
| MSK model | 66.2 ± 13.3 | 125.5 ± 87.6 | 324.4 ± 144.4 | 609.6 ± 161.8 |
| Hybrid model | 54.8 | 193.5 | 418.6 | 718.2 |

Table 5. Cartilage contact pressures at distal interphalangeal (DIP), proximal interphalangeal (PIP) and metacarpophalangeal (MCP) joints estimated by the hybrid model for each of the six subjects and for the average. External fingertip force produced by the hybrid model.

| | | Subject number | | | | | | Average |
|----------------------------------|-------------------------|------------------------------|------------------------------|------------------------------|------------------------------|-------------------------------|-------------------------------|------------------------------|
| | | 1 | 2 | 3 | 4 | 7 | 9 | |
| Cartilage contact pressure (MPa) | DIP joint | $\sigma_{\max} = 19.8$ | $\sigma_{\max} = 26.7$ | $\sigma_{\max} = 26.8$ | $\sigma_{\max} = 31.7$ | $\sigma_{\max} = 32.2$ | $\sigma_{\max} = 44.3$ | $\sigma_{\max} = 33.0$ |
| | | $\sigma_{\text{mean}} = 4.8$ | $\sigma_{\text{mean}} = 6.2$ | $\sigma_{\text{mean}} = 5.7$ | $\sigma_{\text{mean}} = 7.1$ | $\sigma_{\text{mean}} = 7.3$ | $\sigma_{\text{mean}} = 12.2$ | $\sigma_{\text{mean}} = 6.6$ |
| | PIP joint | $\sigma_{\max} = 22.8$ | $\sigma_{\max} = 27.4$ | $\sigma_{\max} = 31.9$ | $\sigma_{\max} = 24.2$ | $\sigma_{\max} = 42.2$ | $\sigma_{\max} = 42.6$ | $\sigma_{\max} = 33.3$ |
| | | $\sigma_{\text{mean}} = 5.9$ | $\sigma_{\text{mean}} = 6.6$ | $\sigma_{\text{mean}} = 7.2$ | $\sigma_{\text{mean}} = 5.8$ | $\sigma_{\text{mean}} = 9.2$ | $\sigma_{\text{mean}} = 7.5$ | $\sigma_{\text{mean}} = 7.8$ |
| | MCP joint | $\sigma_{\max} = 28.9$ | $\sigma_{\max} = 29.1$ | $\sigma_{\max} = 35.9$ | $\sigma_{\max} = 26.1$ | $\sigma_{\max} = 44.3$ | $\sigma_{\max} = 38.4$ | $\sigma_{\max} = 40.4$ |
| | | $\sigma_{\text{mean}} = 6.8$ | $\sigma_{\text{mean}} = 7.1$ | $\sigma_{\text{mean}} = 8.9$ | $\sigma_{\text{mean}} = 6.6$ | $\sigma_{\text{mean}} = 10.0$ | $\sigma_{\text{mean}} = 8.6$ | $\sigma_{\text{mean}} = 9.5$ |
| External fingertip force (N) | $F_{\text{exp}} = 42.5$ | $F_{\text{exp}} = 62.4$ | $F_{\text{exp}} = 65.2$ | $F_{\text{exp}} = 53.5$ | $F_{\text{exp}} = 78.4$ | $F_{\text{exp}} = 64.7$ | $F_{\text{exp}} = 66.2$ | |
| | $F_{\text{sim}} = 36.6$ | $F_{\text{sim}} = 45.7$ | $F_{\text{sim}} = 48.3$ | $F_{\text{sim}} = 39.7$ | $F_{\text{sim}} = 59.6$ | $F_{\text{sim}} = 47.6$ | $F_{\text{sim}} = 54.8$ | |

Supplementary Material A. Tendon forces for the index finger derived from the musculoskeletal model for each of the ten subjects (in N). In bold, the six subjects involved in the analysis.

| | FDP | FDS | LU | RI | UI | EDC | EDI |
|------------------|--------------|--------------|-------------|--------------|------------|-------------|--------------|
| Subject 1 | 71,6 | 126,9 | 5,7 | 117,7 | 0,0 | 50,3 | 64,6 |
| Subject 2 | 93,9 | 123,5 | 4,4 | 139,2 | 0,0 | 59,8 | 76,8 |
| Subject 3 | 84,3 | 94,6 | 14,7 | 194,9 | 0,0 | 90,8 | 116,7 |
| Subject 4 | 125,8 | 49,1 | 0,0 | 152,4 | 0,0 | 44,5 | 57,1 |
| Subject 5 | 99,7 | 210,1 | 0,0 | 149,2 | 0,0 | 67,2 | 86,4 |
| Subject 6 | 113,8 | 281,1 | 4,2 | 262,1 | 0,0 | 141,0 | 181,1 |
| Subject 7 | 107,9 | 234,9 | 0,0 | 190,1 | 0,0 | 79,2 | 101,7 |
| Subject 8 | 102,1 | 177,4 | 12,9 | 245,4 | 0,0 | 124,6 | 160,0 |
| Subject 9 | 217,2 | 46,2 | 9,6 | 161,3 | 0,0 | 72,1 | 92,6 |
| Subject 10 | 81,6 | 236,3 | 0,0 | 199,6 | 0,0 | 126,4 | 162,4 |
| Average | 109,8 | 158,0 | 5,1 | 181,2 | 0,0 | 85,6 | 110,0 |
| SD | 41,0 | 82,2 | 5,6 | 46,3 | 0,0 | 34,1 | 43,8 |

Supplementary Material B. Sensitivity analysis

A sensitivity analysis was performed to investigate the effect of bone material properties and tendon force on the model prediction results. The bone was modelled with three different types of material properties:

- rigid behaviour;
- a single Young's modulus value for all the bone averaged between cortical and cancellous elasticity values;
- distinct cortical and cancellous bone regions (Fig. 3(B))

Tendon force analysis included six cases of tendon force: 100%, 90%, 80%, 70%, 60% and 50% from the baseline values in Supplementary Material A to simulate submaximal grip force levels.

Representing the bone with either rigid behaviour or a single Young's modulus value for all the bone averaged between cortical and cancellous elasticity values led respectively to 11% and 3% higher mean contact pressure at the PIP joint than when distinct cortical and cancellous bone regions were used. All three representations of materials yielded the same values for fingertip force estimation and joint forces. Reducing tendon forces resulted in decreased joint contact pressure, fingertip force, and joint forces. In particular, fingertip force decreased linearly with tendon force (linear correlation of 0.47, $R^2=0.99$) from 54.8 N at maximal tendon force to 25.8 N at halved tendon force. Mean contact pressure also decreased linearly with tendon force (linear correlation of 0.59), from 9.5 MPa, 7.8 MPa, 6.6 MPa at maximal tendon force to 5.5 MPa, 4.9 MPa, 4.2 MPa at halved tendon force for MCP, PIP and DIP joint, respectively.

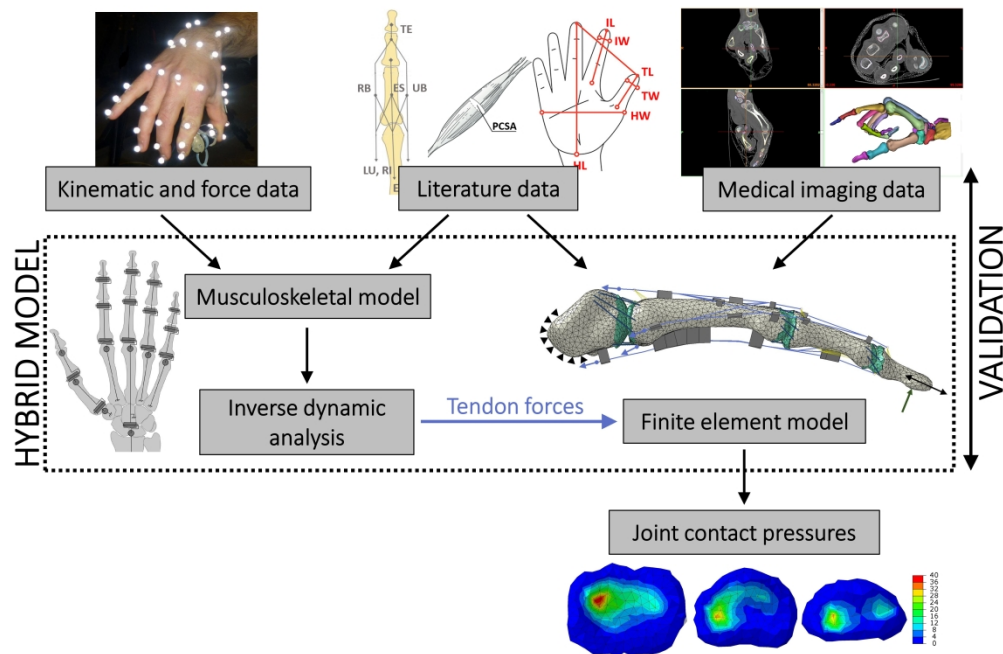


Figure 1. Hybrid musculoskeletal-finite element model applied to the index finger for the estimation of joint contact pressure during a static maximal strength pinch grip task. The musculoskeletal model applied to six subjects estimated tendon and joint forces from motion capture and force data through an inverse dynamic approach. The finite element model based on medical imaging data and including all the major structures of the index finger was driven by tendon forces of the musculoskeletal model. This hybrid approach validated by comparison with experimental data and musculoskeletal results yielded mean and maximal contact pressures at the three index finger joints.

569x379mm (300 x 300 DPI)

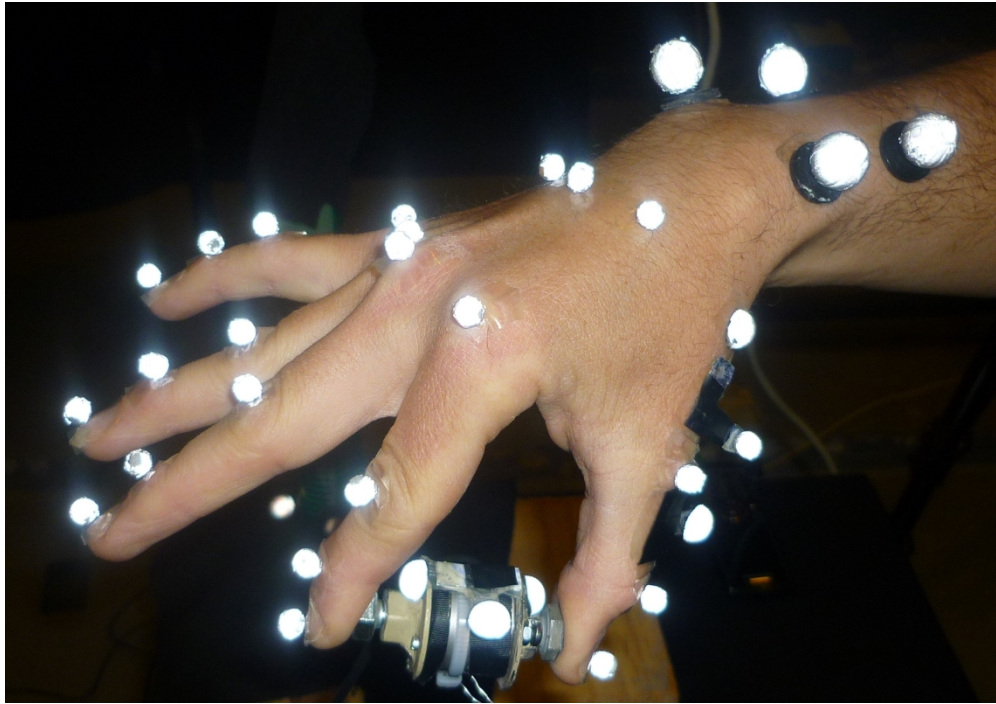


Figure 2. Pulp pinch grip posture and experimental acquisition system. A motion capture system with spherical markers on bony landmarks and an axial force sensor between the thumb and index fingertips were used.

244x171mm (300 x 300 DPI)

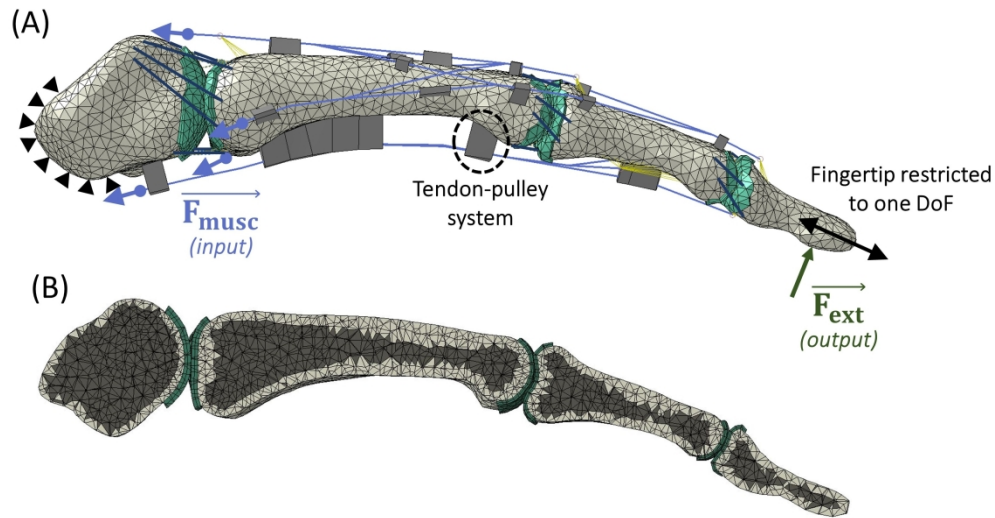


Figure 3. (A) Index finger finite element model of the hybrid approach including bones, cartilage, tendons, annular pulleys and ligaments. Cartilage in green was obtained by extrusion of the bone surfaces with wedge elements. Tendons and annular pulleys in light blue and grey, respectively, were modelled with beam and shell elements, respectively. Ligaments in dark blue were represented by multiple non-linear spring elements. The truncated metacarpal bone was fully constrained and the fingertip restricted to one degree of freedom (DoF) resulting in an external fingertip reaction force (F_{ext}). Datasets of tendon forces (F_{musc}) were applied along the last segment of each tendon. (B) Material properties distribution between cortical (in light grey) and cancellous bone (in black) on a section of the index finger bones.

293x156mm (300 x 300 DPI)

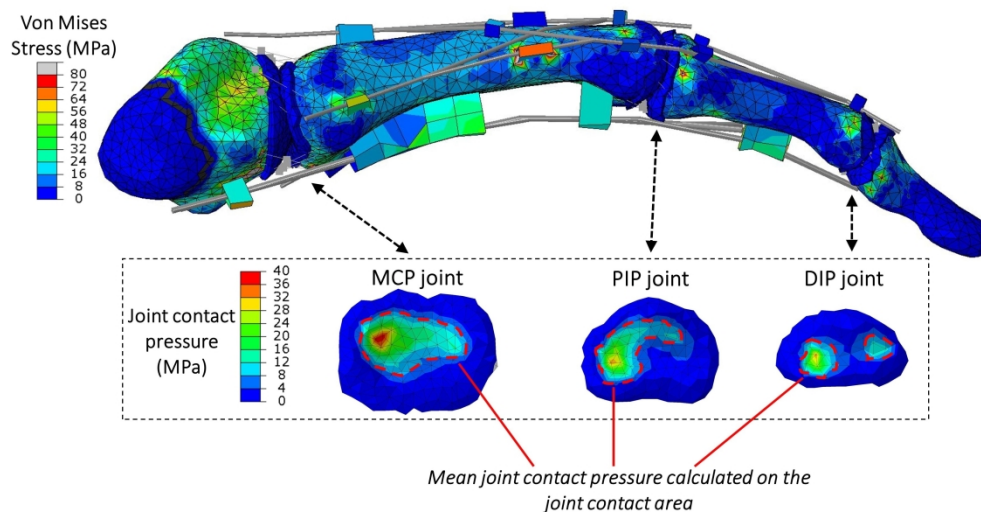


Figure 4. Von Mises stress distribution of the index finger and contact pressure distribution at distal interphalangeal (DIP), proximal interphalangeal (PIP) and metacarpophalangeal (MCP) joints during a static maximal strength pinch grip task applying one dataset of tendon forces.

297x155mm (300 x 300 DPI)